# 4 DEVELOPMENT OF THE SCINTILLATOR DESIGN

## 4.1 A Software Model to Calculate Solid Angle Coverage

Marco Arosio

The aim was to find the solid angle portion of sky that a two-layer coincidence detector covers in order to get an estimate of cosmic ray flux at ground level from our experimental data. The two layer structure of the detector means that it cannot detect particles coming from every direction. The angle of incidence of a "detectable" particle has a maximum value ?. If the particle comes in at an angle bigger than ? it inevitably misses one or both layers.

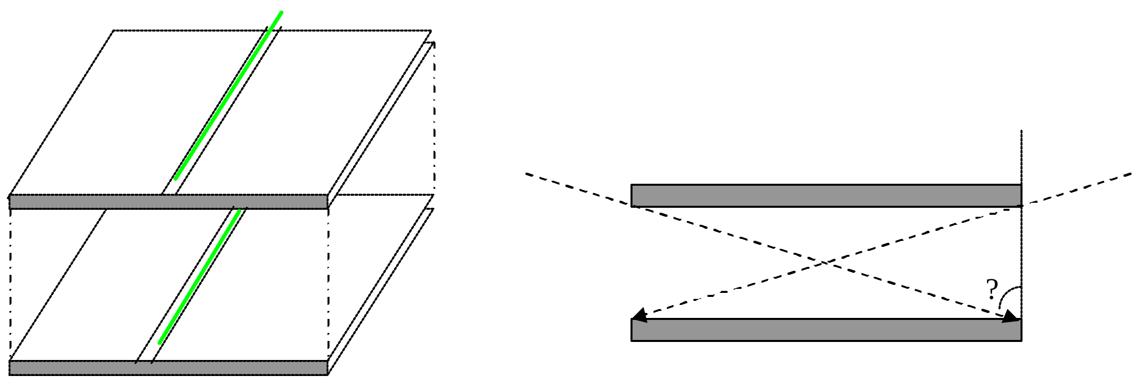


**Figure 52: detector layers and angle of incidence of detectable particles.**

The evaluation of the portion of solid angle covered is complicated by the fact that cosmic rays do not have a common source. Also, the detector is not point-like. An integral result is very difficult to evaluate. The use of a numerical method seemed to be an easier approach.

Random particles scattering from points on the surface of the bottom layer can be simulated and the fraction of these that intersect the top layer calculated. The result gave us an estimate of the fraction of solid angle that a detector of given dimensions would cover.

The bottom layer of the detector was considered and its top surface divided into area elements dA. If the area elements are small enough they can be considered as points (see fig. 53, overleaf). From each point a number of particles (vectors) were produced and scattered in random directions. The fraction of particles that intersected the top insulator layer could then be computed. This operation was done in turn for every point lying on the bottom scintillator and a total overall fraction evaluated . The number of random particles produced per point could be increased in order to improve the accuracy of the result.

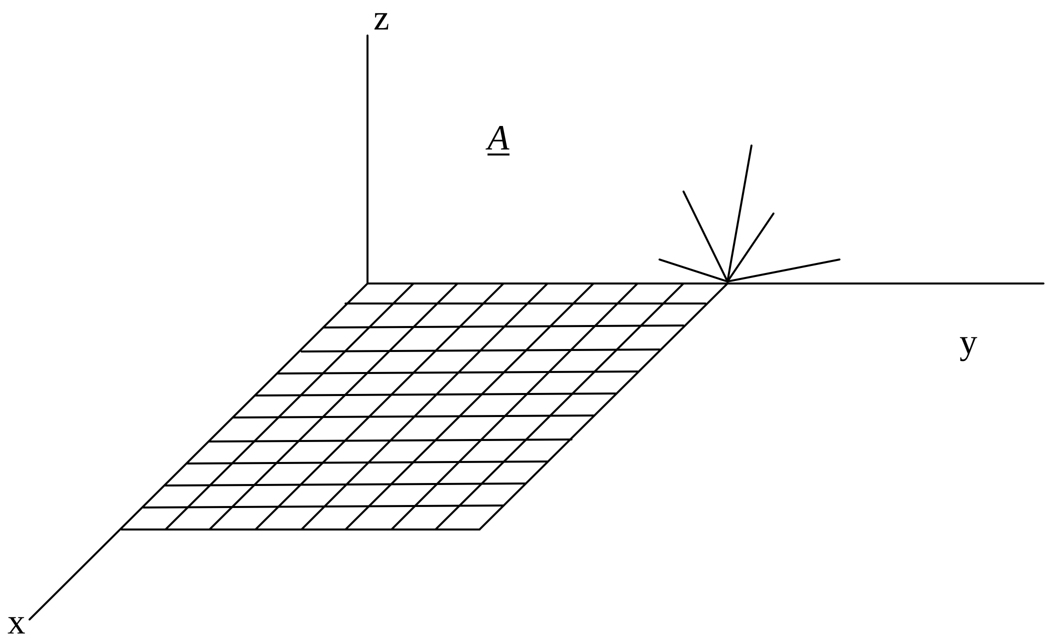


**Figure 53: Bottom layer: each square considered as point source of random particles.**

Components of the random vectors were produced by the generation of random values of the spherical polar coordinates ? and f . Vector components were then calculated as follows:

$$x = r\sin(q)\cos(f)$$

$$y = r\sin(q)\sin(f)$$

$$z = r\cos(q)$$

Values of ? were generated over the range from 0 to p since we are only interested in particles going in the upward direction (with respect to the bottom layer). Values of f were generated over the range from 0 to 2p. Parametric lines of the form $\underline{r} = \underline{P}_0 + \underline{A}t$ were then created for each random vector $\underline{A}$ , where $\underline{P}_0$ defines the location of the origin of the random vector on the insulator surface (see fig. 54, overleaf).

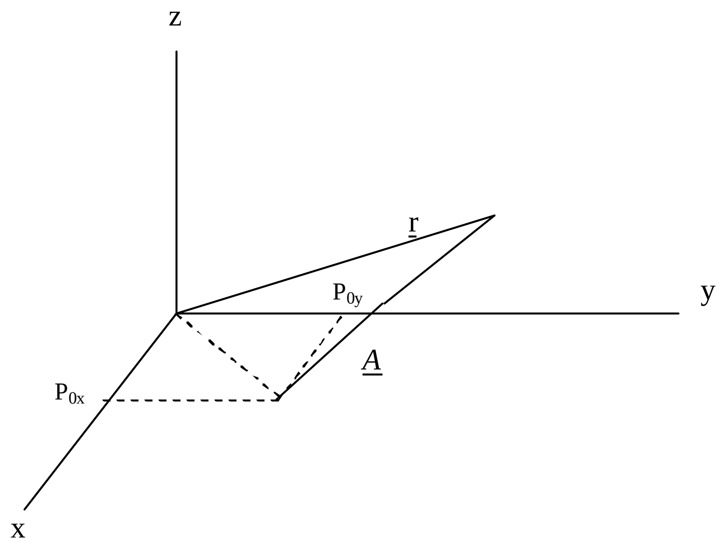


**Figure 54: parametric line r.**

The components of the line in the x, y, and z direction are given by:

$$r_x = P_{o_x} + A_x t$$
$$r_y = P_{o_y} + A_y t$$
$$r_z = P_{o_z} + A_z t$$

The parameter t had to be defined. To do this the fact that condition for which the line intersects the top insulator is that its $r_z$ component is equal to the separation of the insulator layers, d. Also $P_{0x} = 0$ since bottom layer lies in the x-y plane. Therefore

$t = d / A_z$

The line will then be intersecting top layer if x and y components are in the limits:

$0 < x <$ length of insulator

$0 < y <$ width of insulator

Number of random particles generated for each point of the bottom surface could be changed as well as the size of the area elements. The total number of particles generated and total number of intersections of the their trajectory with the top layer could be evaluated and the fraction of “detected” particles determined. This fraction corresponds to the fraction of solid angle covered by the detector.

See Appendix VII for Java code

## 4.2 Testing the Validity of the Solid Angle Calculation

Manuel Kurdian

In order to test the validity of the method in section 4.1 for numerically calculating the solid angle subtended by a detector, the solid angle was calculated for a detector of dimensions given in figure 55. The dimensions are those of the detector used in the SLAC experiment located at Stanford University. Flux and count rate readings were obtained from the SLAC website (see references) from which, the solid angle was calculated. The two values for the solid angle were then compared with each other to deduce whether or not the program developed in section 4.1 could be relied upon to calculate the solid angle subtended by detectors of different dimensions.

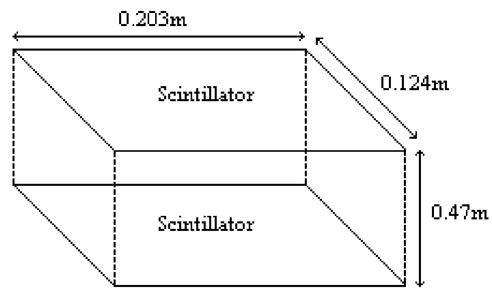


**Figure 55: The dimensions of the SLAC detector**. It is composed of two parallel pieces of equally sized scintillator separated by an air-filled gap.

From the flux and count rate data, the results shown in figure 56, below, were calculated, which are the flux and count rates for different orientations of the detector with respect to the zenith.

| **Orientation of SLAC Detector (degrees from zenith)** | **Flux ($s^{-1}m^{-2}str^{-1}$)** | **Counts ($s^{-1}$)** |
|---|---|---|
| 0 | $96 \pm 1$ | $0.277 \pm 0.003$ |
| 45 | $45.1 \pm 0.7$ | $0.129 \pm 0.002$ |
| 90 | $5.6 \pm 0.2$ | $0.0146 \pm 0.0007$ |

**Figure 56: Table showing the average flux and count rates which were calculated from the SLAC data** (see Appendix VIII).

The uncertainties on the mean of the flux and count rate were assumed to be uncorrelated, and therefore given by equation 7.

$$\left(\Delta \overline{X}\right)^2 = \frac{1}{N} \sum_{i=1}^{N} \left(\Delta X_i\right)^2 \qquad [7]$$

Where $\Delta X_i$ and $\Delta \overline{X}$ are the uncertainties on the individual flux values or count rates, and that on their mean respectively.

The solid angle of the detector was then calculated for each of the orientations by the use of equation 8, which is easily derived from the definition of flux (the number of counts per unit second per unit solid angle):

$$\Omega = \frac{C}{FA} \qquad [8]$$

Where O is the solid angle, C is the count rate, F is the flux and A is the surface area of one of the scintillator pieces.

The values of the solid angle are given in figure 57, below, with their uncertainties given by equation 9.

$$\Delta\Omega = \frac{C}{FA}\sqrt{\left(\frac{\Delta C}{C}\right)^2 + \left(\frac{\Delta A}{A}\right)^2 + \left(\frac{\Delta F}{F}\right)^2} \qquad [9]$$

| **Orientation of SLAC Detector (degrees from zenith)** | **Solid Angle (str)** |
|---|---|
| 0 | $0.115 \pm 0.002$ |
| 45 | $0.114 \pm 0.003$ |
| 90 | $0.104 \pm 0.006$ |

**Figure 57: The values for the solid angle calculated from flux and count rates given in figure2.**

The mean and the uncertainty of the mean solid angle was then calculated by the use of equation 8 to be:

$$\Omega_{SLAC} = 0.111 \pm 0.002\, str \qquad [10]$$

The solid angle calculated by the use of numerical method devised in section 4.1 for the same detector is approximately:

$$\Omega = \quad 0.25\, str \qquad [11]$$

**Summary**

We can be confident with the value [11] as the solid angle of the SLAC detector because the order of magnitude is the same as that of [10]. The reason for the difference most probably may be due to the assumption of 100% for the efficiency scintillators in the computer model, which is not the case in a real situation as for the SLAC detector.

## 4.3 Methods Leading to the Final Geometry

The aim of this section is to show the process through which a final decision was made for the dimensions of the detector.

The decision had been made for the detector to have the form of an octahedral prism, with a pair of scintillators at each octant. This was to allow the detection of cosmic muons incident in the horizontal, 45-degree and vertical directions simultaneously as in figure 58.

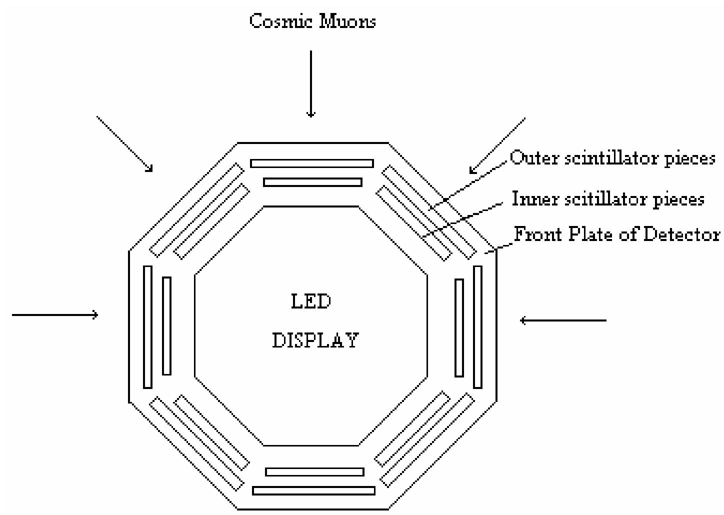


**Figure 58: The layout of the front side of the detector.** This diagram shows the locations of sixteen-scintillator pieces, between which will be an LED display to indicate to the observer the general direction of each detected Muon.

The scintillator pieces are rectangular, their width being governed by the dimensions of the front octagonal plate in figure 58. The length of each of these scintillator pieces was determined in a manner that provided a sufficient count rate that is not too large rendering the individual muon counts indistinguishable, or too small with counts too far apart.

To decide on the width of the inner scintillator pieces, the minimum separation of the opposing inner scintillator surfaces (*d*) was considered. This inner separation was an important factor for the overall size and therefore portability and aesthetics of the detector.

To hold the detector together, it was planned that grooves would be cut onto the front plate to allow the scintillator pieces to slot into them. A small separation was therefore necessary between neighbouring scintillator pieces to avoid structural weakness during machining (see figure 59, overleaf) Due to this separation, the separation *d* of the inner scintillators was increased by 2cm. The values of the separations for a range of widths is given in figure 60, overleaf.

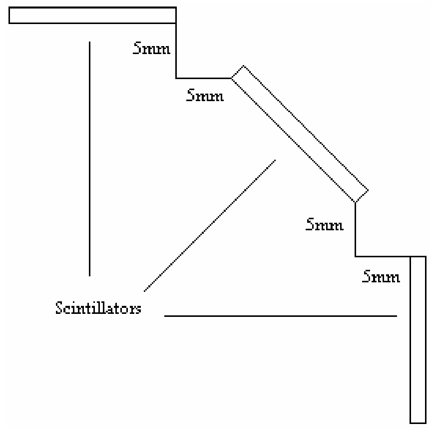


**Figure 59 : A closer view of the method of separation between neighbouring scintillators.**

| **Width of inner scintillator piece (cm)** | **Separation between inner scintillator pieces(cm)** | **Solid Angle (str$^{-1}$)** |
|---|---|---|
| 4 | 11.66 | 0.72 |
| 5 | 14.07 | 0.67 |
| 6 | 16.49 | 0.61 |

**Figure 60: The separation between the inner scintillator pieces for a given range of widths and a length of 17 cm, and their corresponding subtended solid angle.**

For ease of machining of the scintillator pieces and also for the purpose of comparisons with the earlier investigations the length was chosen to be 17cm long. Therefore it was possible to calculate the solid angle subtended by two scintillators in coincidence. The numerical method in section 4.1 was used to do this, the results of which are also given in figure 60.

Before the count rate could be determined in order for a choice for the most appropriate dimensions to be made, a value for the muon flux was required. Two experiments had been performed by the group with two scintillators of different types, where a flux value was determined and given in figure 61.

| **Types of Scintillator** | **Muon Flux Value (str$^{-1}$)** |
|---|---|
| Two old types (experiment 1) | 22.08 |
| One old type, and one new (experiment 3) | 40.57 |

**Figure 61: This table shows the flux values that were obtained for two experiments, one with two pieces of the same type of scintillator, and a second experiment with one scintillator replaces with a new and more efficient type**

If the efficiency of the old scintillator is ‘$e_1$’, and that for the new scintillator is ‘$e_2$’, then the total efficiency ‘$E_{11}$’ of the detector in experiment 1 would be given by [12].

$$E_{11} = e_1^2 \quad [12]$$

The efficiency '$E_{12}$' of experiment 2 would therefore be:

$$E_{12} = e_1 e_2 \approx 2E_{11} \quad [13]$$

The reason for the assumption in [13] is the fact that the flux measured in experiment 2 is roughly double that from experiment 1. Because the accepted value for the flux is 96str$^{-1}$, and the size of the flux values in figure 61, compared with the accepted value are small, we can be confident that the reduction is due to the efficiency of the scintillators used, and therefore the assumption in [13] is reasonable.

To predict a flux value for another experiment two pieces of the new and more efficient scintillator, the efficiency '$E_{22}$' was required, which is given by:

$$E_{22} = e_2^2 \approx 4e_1^2 = 4E_{11} = 2E_{12} \quad [14]$$

According to experiment 1, the expected flux value, by the use of [14] would be:

$$4(22.08) = 88.32 \quad [15]$$

And the flux value according to experiment 2, and by [14] would be:

$$2(40.57) = 81.14 \quad [16]$$

Upper and a lower limits were then calculated from the flux values [14] and [15] by the use of equation [8], and the solid angle values in figure 61, thus giving:

$$C_4 = 0.4 \pm 0.2 s^{-1} \quad [17]$$

$$C_5 = 0.48 \pm 0.02 s^{-1} \quad [18]$$

$$C_6 = 0.53 \pm 0.03 s^{-1} \quad [19]$$

Where $C_4$ corresponds to the count rate for scintillator of width 4 cm, etc.

The dimensions corresponding to $C_5$ were chosen which provides a count approximately every two seconds. Recall that these dimensions are for the inner scintillators.

The dimensions of the outer scintillators were determined in a manner such that the solid angle subtended by the outer scintulllators would have to be equal to or greater than the solid angle of the inner scintillators. This was in order to preserve the minimum count rate given by [18]. Count rate [18] was a minimum because the total solid angle subtended by the whole detector is limited by the smallest scintillators in the path of a cosmic muon, no matter what coincidence mode is used. (The coincidence modes of our detector are 2-way, 3-way, and 4-way).

It was not essential for the outer scintillators to be at a particular separation from the inner scintillator in the same octant, as long as they were separated enough to allow a separation between scintillators of at least that shown in figure 59, p50. The width of the outer scintillators was chosen to be 6.5 cm. The separation (*d1*) of opposing scintillator pieces in an octagon were therefore given by:

$$d1 = 2\left(\frac{6.5}{\sqrt{2}}\right) + 6.5 = 15.69cm \qquad [20]$$

The actual separation (*d2*) would have to be greater than [20], and subtend a solid angle which is greater than or equal to 0.67$str^{-1}$ as given in figure 60.
The separation could not be less than or equal to 17 cm due to the structural reasons mentioned earlier, therefore a separation of 18cm was decided upon which is a compromise since the subtended solid angle is 0.1 $str^{-1}$ less than 0.67 $str^{-1}$as shown by the numerical method in section 4.1.